



Structure of RecX protein complex with the presynaptic RecA filament: Molecular dynamics simulations and small angle neutron scattering



Alexey V. Shvetsov^{a,c,*}, Dmitry V. Lebedev^a, Daria B. Chervyakova^{a,b}, Irina V. Bakhlanova^a,
Igor A. Yung^{a,c}, Aurel Radulescu^e, Aleksandr I. Kuklin^d, Dmitry M. Baitin^{a,c}, Vladimir V. Isaev-Ivanov^a

^a Petersburg Nuclear Physics Institute, NRC Kurchatov Institute, Gatchina, Russia

^b Saint-Petersburg State University, Saint-Petersburg, Russia

^c St. Petersburg State Polytechnical University, St. Petersburg, Russia

^d Joint Centre for Nuclear Research, Dubna, Russia

^e Jülich Centre for Neutron Science Outstation at FRM II, Garching, Germany

ARTICLE INFO

Article history:

Received 24 September 2013

Revised 17 January 2014

Accepted 28 January 2014

Available online 13 February 2014

Edited by Gianni Cesareni

Keywords:

RecX

RecA

Molecular dynamics

GROMACS

Small angle neutron scattering

ABSTRACT

Using molecular modeling techniques we have built the full atomic structure and performed molecular dynamics simulations for the complexes formed by *Escherichia coli* RecX protein with a single-stranded oligonucleotide and with RecA presynaptic filament. Based on the modeling and SANS experimental data a sandwich-like filament structure formed two chains of RecX monomers bound to the opposite sides of the single stranded DNA is proposed for RecX::ssDNA complex. The model for RecX::RecA::ssDNA include RecX binding into the groove of RecA::ssDNA filament that occurs mainly via Coulomb interactions between RecX and ssDNA. Formation of RecX::RecA::ssDNA filaments in solution was confirmed by SANS measurements which were in agreement with the spectra computed from the molecular dynamics simulations.

© 2014 Federation of European Biochemical Societies. Published by Elsevier B.V. All rights reserved.

1. Introduction

The RecA protein is a central enzyme in the recombination complex that ensures homologous recombination and recombination repair in the bacterial cell. Function of RecA involves a search for homology between two DNA molecules and homologous strand exchange. This step is preceded by a presynaptic stage, including cooperative RecA multimerization along ssDNA in the presence of ATP and magnesium ions [1–3]. The structure of the presynaptic complex has been determined by both X-ray crystallography, and, in solution, by SANS. RecA polymer is a helical filament with the pitch of approximately 90–95 Å and ca. 100 Å in diameter [3–5]. Filaments become more abundant on damaged DNA regions in stress, which initiates the so called SOS function of RecA. Expression of more than 40 genes, including the RecA gene, changes as a result of a SOS response. The regulation of RecA by accessory or regulatory proteins is an important aspect of the recombination

process. Interactions with many proteins and protein complexes were shown to exert either activating or inhibiting effects on RecA filamentation. These proteins can be classified as positive and negative regulators, although this division is rather arbitrary because some of the proteins inhibit certain functions of the filament while activating the others. Much of the regulation is focused on RecA filament assembly and disassembly [6–9]. RecX acts as a negative regulator of RecA both in vivo and in vitro. The gene encoding the regulatory protein RecX in *Escherichia coli* was discovered by Zaitsev et al. [10] which was designated then as *oraA*. Lately this gene was identified as the RecX encoding sequence [11]. Seifert and co-workers [9] demonstrated that RecA and RecX proteins physically interact using yeast two-hybrid analysis. It was demonstrated that RecX interacts directly with RecA, thus preventing elongation of the filament and making it to dissociate from ssDNA [12]. Several models were advanced to explain the suppression of RecA filamentation by RecX. According to one model, RecX finds a gap in the filament, binds to the nearest monomer, and interrupts monomer polymerization along the DNA strand. The dynamics of monomer dissociation from the 5' end of the filament remains unchanged, while filament assembly is terminated, that is, filament extension by adding new monomers to the 3' end stops [12].

* Corresponding author at: Petersburg Nuclear Physics Institute, NRC Kurchatov Institute, Gatchina, Russia.

E-mail addresses: alexxy@omrb.pnpi.spb.ru (A.V. Shvetsov), dtry@omrb.pnpi.spb.ru (D.V. Lebedev).

Another model suggests that RecX interacts with RecA monomers spontaneously along the total filament to provoke RecA dissociation at the interaction sites [13]. Some RecA mutant proteins are less inhibited by RecX protein. There is only a slight decrease in the rate of ATP hydrolysis of the RecA Δ C17 protein or RecAD112R protein at high RecX concentration [14,15]. Previously we showed that RecX and SSB act as functional antagonists; i.e., the inhibitory effect of RecX on RecA decreases substantially in the presence of SSB [16]. A decrease is observed regardless of the order of adding the proteins to the reaction mixture and is reversible. Since RecX–SSB protein–protein interactions were not detected and SSB does not interact with RecA, the regulation seems to involve DNA regions located either within or immediately outside the filament. The interaction of RecX with DNA was indeed demonstrated in several studies, but RecX affinity for DNA is relatively low [12,17]. On the other hand the recent results suggest that the RecX *Herbaspirillum seropedicaes* (Hs) protein negatively modulates the RecA Hs activities by both protein–protein and DNA–protein interactions [18].

2. Materials and methods

2.1. Molecular modeling of RecA::ssDNA and RecA::ssDNA::RecX complexes

Two RecA::ssDNA presynaptic complex models containing 12 and 33 RecA monomers and ATP were built based on the existing RecA::ssDNA crystal structure pdbid: 3CMW [19,20,3]. Each monomer in this structure was replaced by full length RecA from *E. coli* monomer containing residues 2–334 of the original *E. coli* RecA sequence. Missing parts of the X-ray structure were built using homology modeling tools from ICM [21,22]. A 42 dT oligonucleotide was used in a 12-mer model and a 102-base oligonucleotide (three repeats of 5'-TCA CCA ATG AAA CCA TCG ATA GCA GCA CCG TAA T-3') was used in the long filament.

The structure of RecX monomer (pdbid: 3C1D [13]) with the missing C- and N-terminal residues added using ICM (Fig. 1 left) together with the 12-mer RecA presynaptic complex model were used to build the starting structure of the complex for MD simulation using protein–protein docking technique available in ICM package [21,22].

2.2. Modeling of RecX::ssDNA complex

The structure of RecX protein (pdbid: 3C1D [13]) available from PDB with the missing C- and N-terminal residues added by ICM and a 42 dT oligonucleotide were used as the starting structures for RecX::ssDNA complex.

2.3. Molecular dynamics simulation of RecA::ssDNA and RecA::ssDNA::RecX complexes

All MD simulations was performed in GROMACS [23–26] software package using amber99sb-ildn [27] force field for protein and DNA, and tip3p [28] model for explicit water. Simulated systems were around 700 k atoms in size including explicit solvent shell and 150 mM NaCl to neutralize charge on protein and dna. Solvent shell thickness was 1.5 nm or higher. System was equilibrated using two step protocol. During the first step the system was equilibrated during 10 ns with all heavy protein atoms restrained to their initial position using NPT ensemble. During the second step the system was equilibrated without restrains for 10 ns starting from the last frame from the previous step. After two equilibration stages 100 ns trajectory was simulated with a time step of 2 fs. Neighbor search was performed every 50 steps. The S-PME algorithm was used for electrostatic interactions with a cut-off of 1.2 nm. A cut-off of 1.2 was used for Van der Waals interactions. Temperature coupling was done with the Nose–Hoover algorithm at 310 K. Pressure coupling was done with the Parrinello–Rahman algorithm for 1 bar.

2.4. Calculation of SANS spectra from MD

To calculate SANS spectra from MD trajectory we used GROMACS g_sans [29] tool enhanced to support MD trajectory averaging. Since scattering intensity can be written as [30]

$$S(\vec{q}) = \int G(\vec{r}) e^{i\vec{q}\vec{r}} d\vec{r} \quad (1)$$

which can be rewritten in case of molecule in solution using Debye formula as

$$S(q) = \int G(r) \frac{\sin qr}{qr} dr \quad (2)$$

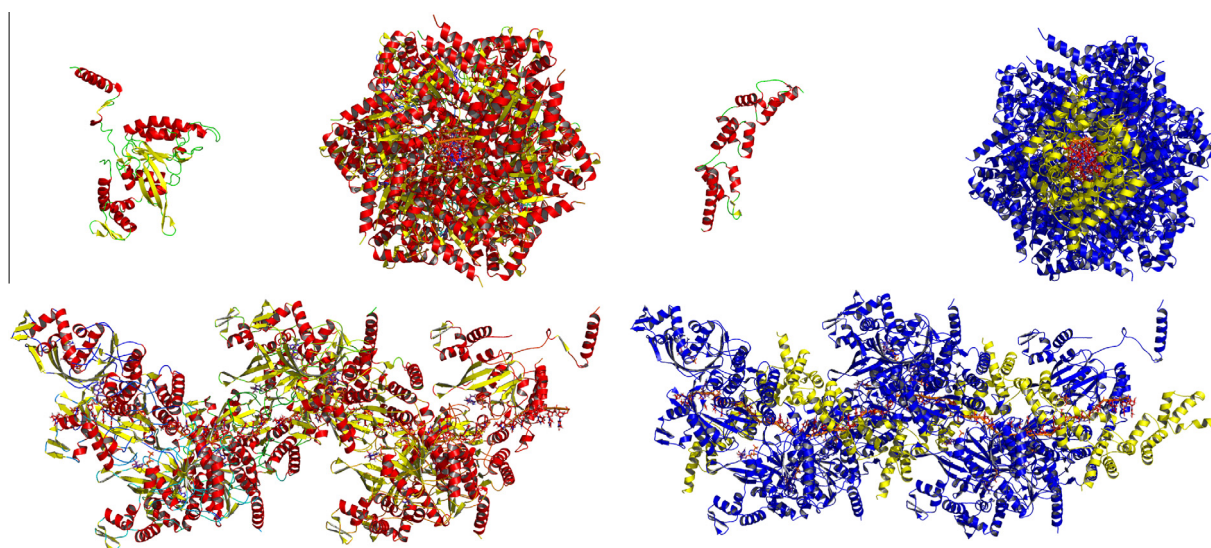


Fig. 1. Reconstruction of full-atom structure of RecA and RecX monomers and models for RecA::ssDNA (left) and RecA::RecX::ssDNA (right) complexes. For both sets top-left corner shows the monomer structure with the missing unstructured regions reconstructed; top-right corner and bottom structures are the two projection view of the polymers. In RecA::RecX::ssDNA complex 5 RecX protein monomers (shown in yellow) are located in the groove of RecA helical 12-mer (shown in blue).

where the radial distribution function $G(r)$ for the trajectory frame can be calculated as

$$G(r) = \sum_{i,j} b_i b_j \quad (3)$$

$$r = \|\vec{r}_i - \vec{r}_j\|$$

where b_i and b_j are scattering length for particles i and j that can be found online or in Sears et al. [31]. $G(r)$ was averaged over all time frames gathered from MD trajectory to take into account the fact that macromolecular complex was not static. After that $S(q)$ was calculated by Eq. 2.

2.5. Expression and purification of RecA and RecX proteins

E. coli RecA was purified from the strain JC10289 with the relevant genotype $\Delta recA thr-1 leu-6 Str^r$ [32] carrying the wild type *recA* gene under its own promoter within the plasmid pUC19-*recA*1.1 [33]. The cells were grown at 37 °C in 2 l of Luria–Bertani medium in the presence of 100 µg/ml ampicillin to an OD_{595} of 0.6 and the protein expression was induced for 3 h by the addition of nalidixic acid (50 µg/ml). Cells were harvested by centrifugation at +4 °C. The cell paste was suspended in cold 250 mM Tris–HCl (pH 7.5), 25% sucrose, frozen in liquid nitrogen and stored at –70 °C. All further manipulations of RecA protein purification were conducted according to the standard procedure as described elsewhere [34] with slight modifications. The protein was dialyzed into the storage buffer on D₂O, containing 20 mM Tris–HCl, pH 7.5, 1 mM DTT, and 50% (w/v) glycerol and stored at –20 °C. The RecA protein concentration was determined by absorbance at 280 nm, using an extinction coefficient of $2.23 \cdot 10^4 \text{ M}^{-1} \text{ cm}^{-1}$ [35]. The plasmid pEAW224 originated from pET21d (Novagen) containing the *E. coli* *recX* gene under the T7 RNA polymerase promoter and the host strain STL327/pT7pol26 [14] were kindly provided by Prof. M.M. Cox (Wisconsin University, US). Four liters of cells STL327/pT7pol26 transformed with pEAW224 were grown to an OD_{595} of 0.6 and the expression of RecX was induced for 3 h by the addition of IPTG to final concentration of 0.5 mM. The cells were harvested and stored as in RecA isolation procedure. All following steps were carried out in concordance with the previously described procedure [14] with slight changes. Since RecX protein does not well endure procedures of freeze/defrost it was kept precipitated in 2.9 M ammonium sulfate solution at +4 °C and dialyzed into the storage buffer on D₂O, containing 20 mM Tris–HCl, pH 7.5, 1 mM DTT, 0.1 mM EDTA, 150 mM KCl and 50% (w/v) glycerol just before an experiment. The concentration of the RecX protein was determined from the absorbance at 280 nm using the extinction coefficient $2.57 \cdot 10^4 \text{ M}^{-1} \text{ cm}^{-1}$ [36]. All reagents were purchased from world-wide well-known companies (Sigma–Aldrich, Pancreac, AppliChem) and were of the highest grade available.

2.6. SANS measurement

Presynaptic RecA filaments were assembled on a single-stranded oligonucleotide (added at slight excess to the molar ratio of 3.6 nucleotides per one RecA molecule) 102 bases in length (three repeats of 5'-TCA CCA ATG AAA CCA TCG ATA GCA GCA CCG TAA T-3') and stabilized by the presence of a non-hydrolyzable ATP analog (2 mM ATP γ S) and 10 mM MgCl₂, in accordance with the earlier biochemical studies [36]. RecX stock (D₂O Tris–HCl buffer/50% glycerol) was added to the sample containing either pure oligonucleotide, or the presynaptic complex. The final concentration in the samples (calculated from the protein stock dilution) were 150 mM for RecA and 60 mM for RecX protein. SANS spectra were registered on JuMO spectrometer (IBR-2 reactor, Dubna, Russia, preliminary measurements) and on KWS-2 spectrometer

at FRM-2 reactor (Garching, Germany). The measurements were performed in 95% D₂O 5% glycerol Tris–HCl buffer pH 7.5 at 15 °C with the exposure times between 5 and 60 min.

3. Results and discussion

Based on the existing RecA::ssDNA crystal structure [3] we built RecA::ssDNA presynaptic complex models for a short filament containing 42 dT nucleotides and a longer filament containing 102-base oligonucleotide. Unlike RecA homopolymer [37], neither of the modeled filaments has shown any substantial changes in its structure during 100 ns molecular dynamics simulation, except for some minor motions of the C-terminal domain and in L1 and L2 loops regions that have contacts with ssDNA.

To model RecX::ssDNA complex we have noticed that the RecX crystal has $P2_12_12_1$ symmetry group and the asymmetric unit contains dimer. Using symmetry data to built crystallographic neighbors we observe that they can form a chain of head-to-tail RecX dimers that has positively charged surface from one side of chain (Fig. 2). We further assumed that two such bend-like RecX filaments can bind to ssDNA from both sides and form sandwich-like structure (Fig. 3 top two views). MD simulation shows that RecX::ssDNA filaments should be quite flexible with persistent length near 200 Å.

While no X-ray structure of RecA::RecX complex exist at this moment, the low resolution structure based on Cryo-EM [38] shows that RecX should likely bind to the RecA::ssDNA complex filament groove. During modeling phase we prepared 3 models with different stoichiometries of RecX:RecA ratio (2:12, 3:12, 5:12). All of this models were stable during production MD (100 ns simulations as mentioned in Section 2).

Small angle neutron scattering experiment was performed to obtain the information on the low-resolution structure of RecX::RecA::ssDNA complex in solution, and to test whether molecular model of such an interaction is supported by experiment.

The spectrum of the presynaptic complex (Fig. 4, squares) showed the typical for rod-like particles $1/q$ dependency in the low scattering angles and the local minimum near 0.07 \AA^{-1} and a maximum near 0.09 \AA^{-1} . This scattering pattern was similar to that observed in the earlier SANS studies of RecA protein filaments [4,5] where this feature of the spectrum was associated with the helix periodicity. The position of the minimum (real space length of 90 Å) is close to that expected for the stretched form of RecA filament, corresponding to the presynaptic complex. In the range of scattering vector magnitudes above 0.02 \AA^{-1} the experimental spectrum fit very well to the MD simulation for the complex of 33 RecA molecules with 102-long single stranded oligonucleotide (Fig. 4, solid line). The spectra obtained from the single frame of the trajectory (pre-equilibrated structure) showed poorer fit to the experimental data.

The absolute values of the scattering intensity imply that approximately 60% of RecA protein added to the experimental sample was recruited into the filament. This value is rather low, considering very good RecA recruitment into the presynaptic complex has been reported earlier [36] even at much lower protein concentrations. It appears more likely that we underestimate the amount of RecA filaments (due to uncertainties in excluded volume estimate) and/or overestimate the total amount of RecA in the sample available for binding (due to a combination of experimental errors such as uncertainties in extinction coefficient, OD determination, protein impurity, aggregation, etc.). In the range of the scattering vector magnitudes $0.02\text{--}0.05 \text{ \AA}^{-1}$ the data can be linearized in the appropriate Guinier coordinates (Fig. 5C, squares), yielding the cross-sectional gyration radius of the filament R_c of $33.9 \pm 0.1 \text{ \AA}$, which is very close to 33.8 \AA expected from

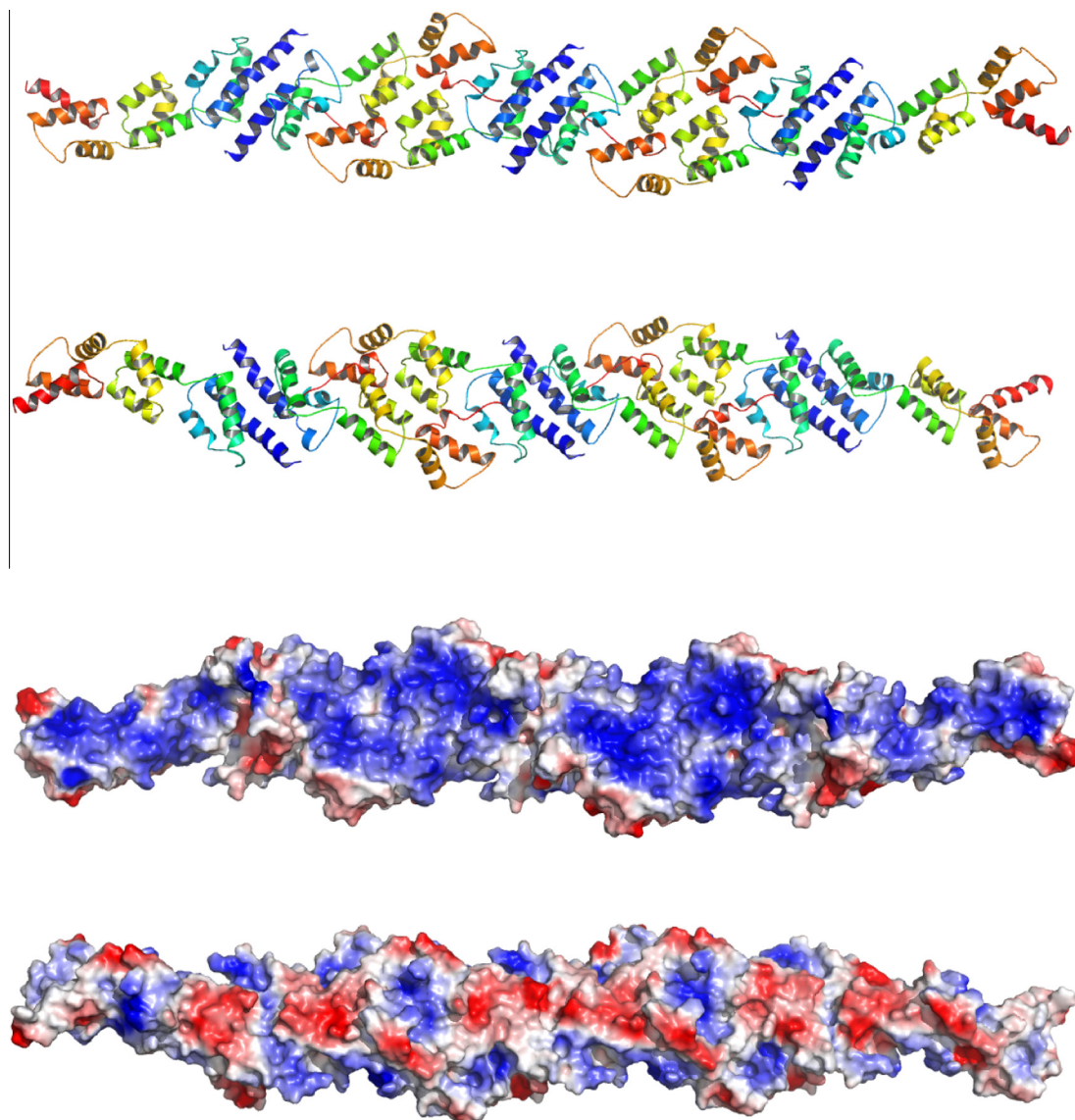


Fig. 2. Structure of RecX chains. Chains comprised by six RecX monomers were assembled based on the available X-ray structure (see text). Cartoon view of two chains mutually rotated 180 degrees along the main axis (top) and their electrostatic potential (bottom): positive charges colored blue, negative red.

the model. The $1/q$ behavior of the experimental curves extended much further into the small angle region than predicted by the simulation, pointing to the rod-like particles that were much longer than expected for the presynaptic RecA complex with 102-base oligonucleotide. In the region of $q < 0.02 \text{ \AA}^{-1}$ there appears to be another linear region with the slope corresponding to $R_c=62 \text{ \AA}$. Most likely we observed the formation of the longer rod-like bundles, composed of the shorter presynaptic 102-base oligonucleotide fragments, and some larger aggregates.

RecX interaction with the presynaptic complex did not affect the rod-like shape of RecA polymer (Fig. 5A, triangles). The length of the rods continued to exceed the expected length of the stretched 102-nucleotide ssDNA, but the rise in intensity in the low scattering angles was smaller (Fig. 5C), pointing to the likely decrease in the bundle formation. The cross-sectional gyration radius was the same as for the presynaptic filament ($34.1 \pm 0.1 \text{ \AA}$). At the same time, RecX addition significantly reduced the pattern of 0.07 \AA^{-1} minimum and the local maximum. Considering that RecX contributes only 20% to the protein mass, this effect of RecX was much larger than would be expected from a mere addition of scattering from a RecX filament on a single-stranded oligonucleotide

(Fig. 5A, circles), indicating that complex formation between RecX and RecA filament took place.

We have compared the experimental data with the scattering simulated from the model structures corresponding to three different stoichiometric ratios of RecX in the filament (Fig. 5B, broken lines). All three models suggest that RecX binding decrease the magnitude of the diffraction peak and had little effect on the filament gyration radius ($33\text{--}34 \text{ \AA}$). The model with RecX:RecA stoichiometric ratio of 3:12 (Fig. 5B, dash-dot line) appear to be in the best agreement with the experimental data.

Comparison of the spectrum of RecX protein in the presence of ssDNA with those calculated from two RecX:ssDNA models clearly shows that the sandwich-like model with the stoichiometry of one RecX per six nucleotides has a very good agreement with the experiment in the large angle region ($q > 0.02 \text{ \AA}^{-1}$, Fig. 5A, dash-dot line).

The scattering intensity shows that ca. 50% of RecX present was bound to DNA. Similar to RecA protein estimate, we may expect this value to be underestimated. Experimental data in the smaller q follows the power law with the exponent close to -2 (Fig. 5A, dashed line), indicating that RecX:ssDNA filaments are flexible on

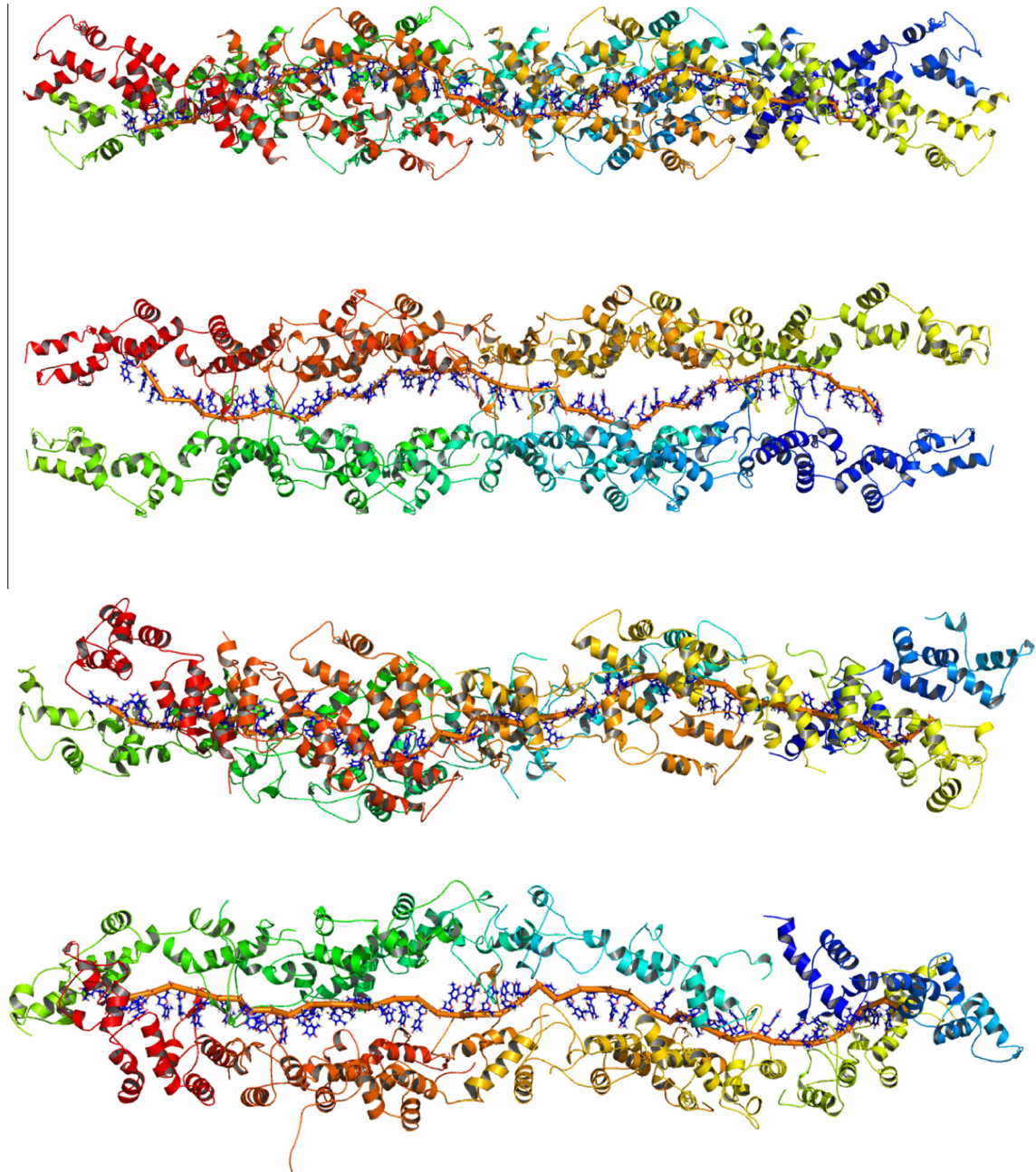


Fig. 3. Full-atomic model for RecX::ssDNA sandwich-like filament: starting structure of protein chains (two chains of six monomers each, ribbons) bound to the opposite sides of DNA (top) and the same structure after 100 ns of MD (bottom). Two orthogonal longitudinal projections are shown.

the scale well below 500 Å and can bind together forming gaussian aggregates.

To look into the possible molecular mechanisms of interaction between RecX and the presynaptic complex, MD simulations were used to calculate the contact map of RecX monomers. Such a map, averaged over 100 ns trajectory and all RecA and RecX monomers (Fig. 7), shows that RecX has contacts (8–10 Å) with RecA only in L1 and L2 loops regions (residues 155–170 and 195–205 respectively) also it has contacts with α -helices 1 (residues 3–21) and 7 (residues 122–135) that forms inter subunit interface in filament near polymerization motif β -sheet 0 (residues 38–41) near L1 loop. We found no contacts at all with RecA C-terminal domain (with distances <15 Å) which were hypothesized earlier by Van Look et al. [38] based on their Cryo-EM studies. It therefore seems questionable whether the general proximity of C-terminal domain

based on low-resolution Cryo-EM structure results in actual interactions between RecX and C-terminal domain of RecA. At the same time, the averaged contact map shows that there are several persistent contacts of RecX with DNA in the same regions where contacts with RecA loops were found, particularly around the positively charged amino acid residues R17 R20 R25 H27 R33 K35 R91 R93 K140 R150 as well as R162 (Fig. 6oat>). This would suggest that for RecA::RecX::ssDNA complex RecX mostly interacts with ssDNA via unspecific coulomb interactions of charged nucleic acids exposed to its positively charged surface. For RecX::ssDNA sandwich-like filament complex the contact map again shows that there mostly non-specific coulomb interactions occur between RecX and ssDNA (Fig. 8) in the same regions as for RecA::RecX::ssDNA filament. Molecular dynamics simulation suggests that DNA in the sandwich-like RecX::ssDNA complex is noticeably

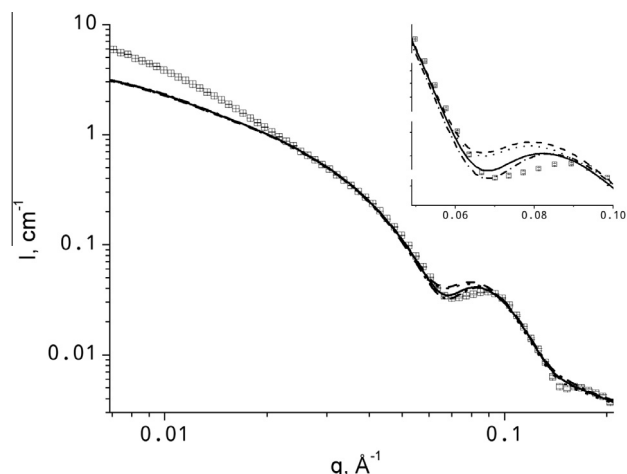


Fig. 4. SANS spectrum of RecA complex with ssDNA (presynaptic complex). Lines show the model spectra calculated from MD simulation of RecA::ssDNA::ATP complex by GROMACS *g_sans* [29] tool with (solid) and without (dash-dot line) taking DNA contribution into account, and from the starting (10 ns equilibrated) structure of MD by CRYSON [39] (dashed) and GROMACS utility *g_sans* (dot line). Data were fitted to the simulated spectra in the range $0.02\text{--}0.2\text{ \AA}^{-1}$ to adjust for incoherent background and protein concentration.

stretched (5.5 \AA per base in RecX::ssDNA), as compared to the other complexes (5.0 \AA in the half-sandwich RecX::ssDNA and 4.9 \AA in RecA::ssDNA filaments).

The presented SANS experiment results strongly suggest that complexes of RecX protein with ssDNA and with the presynaptic RecA filament are formed in solution. The proposed full atomic models for RecX complexes are consistent with SANS data. The molecular dynamics simulations yield the persistent contacts of RecX with ssDNA as well as with the regions of RecA near the monomer–monomer interface. These interactions could result in RecX blocking RecA polymerization on ssDNA when it binds at the end of the presynaptic filament, as suggested earlier [12,36].

Our results imply a major role of RecX–DNA interactions in the protein function. While the reported values for the affinity of RecX to DNA are relatively low [12,17], it is possible that the RecX–DNA

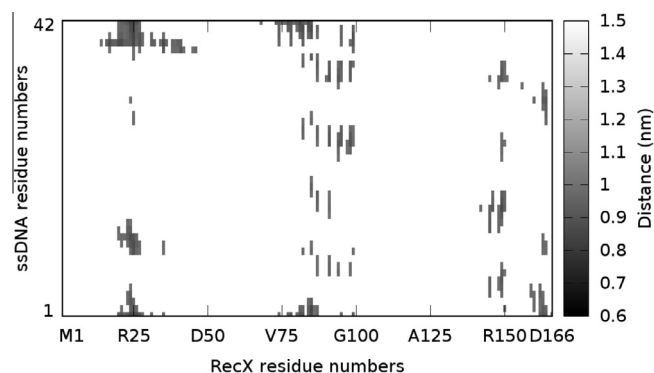


Fig. 6. Contact maps for RecX and ssDNA in RecA::RecX::ssDNA complex.

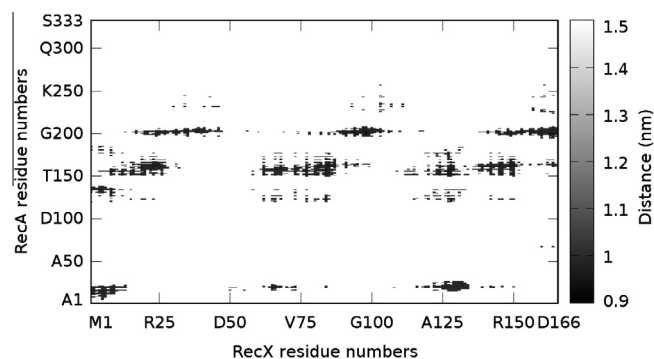


Fig. 7. Contact maps for RecX and RecA in RecA::RecX::ssDNA complex.

interaction is strengthened allosterically by the RecA filament. Stretching of ssDNA by RecX seen in the molecular dynamics model indicate that extended conformation of ssDNA (as in the presynaptic complex) may provide some gain in entropic free energy term for RecX binding, so that the RecX affinity to ssDNA in the presynaptic complex may be higher than in bulk solution. As a consequence, it appears possible that RecX could have an ability to destabilize the presynaptic filament. Higher RecX affinity to the

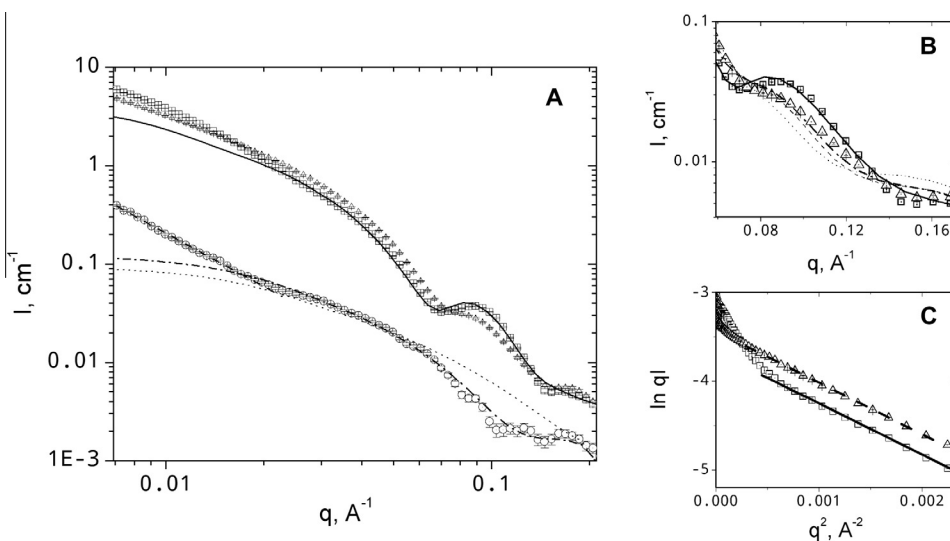


Fig. 5. SANS spectra of RecA and RecX complexes: (A) squares – RecA with ssDNA (presynaptic complex), triangles – same complex with RecX present, circles – RecX complex with ssDNA. Lines show the model spectra calculated from MD simulation of RecA::ssDNA::ATP complex (solid), one-sided (dotted) and sandwich-like (dash-dot line) RecX::ssDNA complex; dashed line show the fit of small q experimental data to the power law dependency with the exponent of -2 . (B) The spectrum region near the diffraction maximum; lines show the spectra for RecX complex with RecA presynaptic filament simulated at RecX:RecA ratios of 0 (no RecX, solid line), 2:12 (thin dashed line), 3:12 (dash-dot line) and 5:12 (thin dot line). (C) Guinier region of the presynaptic filament and its complex with RecX; linear fit for the region $0.02\text{--}0.05\text{ \AA}^{-1}$.

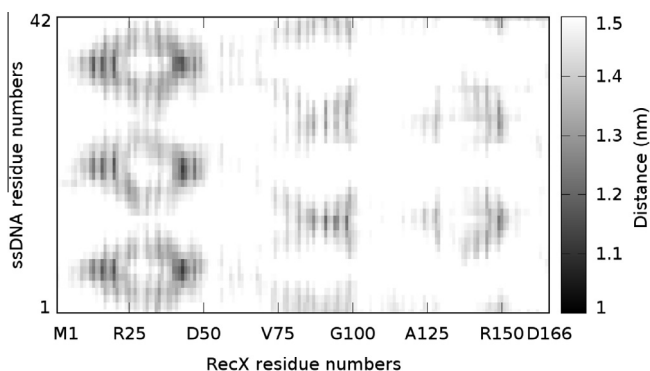


Fig. 8. Contact maps for RecX and ssDNA in RecX::ssDNA complex.

extended ssDNA may also facilitate RecX interaction with the post-synaptic strand of ssDNA in the process of homologous recombination.

4. Conclusions

Small angle neutron scattering experiment together with molecular modeling shows that in solution RecX can form sandwich-like filaments on ssDNA and can bind to RecA::ssDNA::ATP γ S complex without destruction of its filament structure. Based on these results we propose a molecular model of RecX complex with RecA presynaptic filament where RecX protein binds in the filament groove at RecX:RecA molar ratio close to 1:4. The model implies RecX binding mainly via Coulomb interactions between RecX and ssDNA inside the filament similar to ssDNA–RecX.

Competing interests

The authors declare no conflict of interest.

Authors' contributions

All authors read and approved the final paper.

Acknowledgements

This work is based upon experiments performed at the KWS-2 instrument operated by JCNS at the Heinz Maier-Leibnitz Zentrum, Garching, Germany. The work was funded in part by RFBR grants 11-04-01229-a, 14-04-00817a and 12-02-12053-ofi-m and by Federal Program of the Russian Ministry of Education and Science “Using neutron spectroscopy and full-atomic molecular modeling for understanding of DNA compactization in living cells” 07.09.2012 N^o 8482. The results of the work were obtained using computational resources of MCC NRC “Kurchatov Institute” (<http://computing.kiae.ru/>). We acknowledge with gratitude to Prof. M.M. Cox and his research group for providing plasmids and strains necessary for proteins isolation.

Appendix A. Supplementary data

Supplementary data associated with this article can be found, in the online version, at <http://dx.doi.org/10.1016/j.febslet.2014.01.053>.

References

[1] Roca, A.I. and Cox, M.M. (1990) The recA protein: structure and function. *Crit. Rev. Biochem. Mol. Biol.* 25 (6), 415–456, <http://dx.doi.org/10.3109/10409239009090617>.

[2] Kowalczykowski, S.C. (2000) Initiation of genetic recombination and recombination-dependent replication. *Trends Biochem. Sci.* 25 (4), 156–165, [http://dx.doi.org/10.1016/S0968-0004\(00\)01569-3](http://dx.doi.org/10.1016/S0968-0004(00)01569-3).

[3] Chen, Z., Yang, H. and Pavletich, N.P. (2008) Mechanism of homologous recombination from the recA-ssDNA/dsDNA structures. *Nature* 453 (7194), 489, <http://dx.doi.org/10.1038/nature06971>.

[4] DiCapua, E., Schnarr, M., Ruigrok, R.W., Lindner, P. and Timmins, P.A. (1990) Complexes of recA protein in solution: a study by small angle neutron scattering. *J. Mol. Biol.* 214 (2), 557–570, [http://dx.doi.org/10.1016/0022-2836\(90\)90198-U](http://dx.doi.org/10.1016/0022-2836(90)90198-U).

[5] Lebedev, D., Baitin, D., Islamov, A., Kuklin, A., Shalguev, V., Lanzov, V. and Isaev-Ivanov, V. (2003) Analytical model for determination of parameters of helical structures in solution by small angle scattering: comparison of recA structures by {SANS}. *FEBS Lett.* 537 (1–3), 182–186, [http://dx.doi.org/10.1016/S0014-5793\(03\)00107-8](http://dx.doi.org/10.1016/S0014-5793(03)00107-8).

[6] Shan, Q., Bork, J.M., Webb, B.L., Inman, R.B. and Cox, M.M. (1997) RecA protein filaments: end-dependent dissociation from ssDNA and stabilization by recO and recR proteins. *J. Mol. Biol.* 265 (5), 519–540, <http://dx.doi.org/10.1006/jmbi.1996.0748>.

[7] Lusetti, S.L., Voloshin, O.N., Inman, R.B., Camerini-Otero, R.D. and Cox, M.M. (2004) The dini protein stabilizes recA protein filaments. *J. Biol. Chem.* 279 (29), 30037–30046, <http://dx.doi.org/10.1074/jbc.M403064200>.

[8] Galkin, V.E., Britt, R.L., Bane, L.B., Yu, X., Cox, M.M. and Egelman, E.H. (2011) Two modes of binding of dini to recA filament provide a new insight into the regulation of sos response by dini protein. *J. Mol. Biol.* 408 (5), 815–824, <http://dx.doi.org/10.1016/j.jmb.2011.03.046>.

[9] Stohl, E.A., Brockman, J.P., Burkle, K.L., Morimatsu, K., Kowalczykowski, S.C. and Seifert, H.S. (2003) *Escherichia coli* recX inhibits recA recombination and coprotease activities in vitro and in vivo. *J. Biol. Chem.* 278 (4), 2278–2285, <http://dx.doi.org/10.1074/jbc.M210496200>.

[10] Zaitsev, E., Alexseyev, A., Lanzov, V., Satin, L. and Clark, A.J. (1994) Nucleotide sequence between recA and alsp in *E. coli* {K12} and the sequence change in four recA mutations. *Mutat. Res. Lett.* 323 (4), 173–177, [http://dx.doi.org/10.1016/0165-7992\(94\)90030-2](http://dx.doi.org/10.1016/0165-7992(94)90030-2).

[11] De Mot, R., Schoofs, G. and Vanderleyden, J. (1994) A putative regulatory gene downstream of recA is conserved in gram-negative and gram-positive bacteria. *Nucleic Acids Res.* 22 (7), 1313–1314, <http://dx.doi.org/10.1093/nar/22.7.1313>.

[12] Drees, J.C., Lusetti, S.L., Chitteni-Pattu, S., Inman, R.B. and Cox, M.M. (2004) A recA filament capping mechanism for recX protein. *Mol. Cell* 15 (5), 789–798, <http://dx.doi.org/10.1016/j.molcel.2004.08.026>.

[13] Ragone, S., Maman, J.D., Furnham, N. and Pellegrini, L. (2008) Structural basis for inhibition of homologous recombination by the recX protein. *EMBO J.* 27 (16), 2259–2269, <http://dx.doi.org/10.1038/emboj.2008.145>.

[14] Drees, J.C., Lusetti, S.L. and Cox, M.M. (2004) Inhibition of recA protein by the *Escherichia coli* recX protein: modulation by the recA c terminus and filament functional state. *J. Biol. Chem.* 279 (51), 52991–52997, <http://dx.doi.org/10.1074/jbc.M409050200>.

[15] Bakhlanova, I.V., Dudkina, A.V., Baitin, D.M., Knight, K.L., Cox, M.M. and Lanzov, V.A. (2010) Modulating cellular recombination potential through alterations in recA structure and regulation. *Mol. Microbiol.* 78 (6), 1523–1538, <http://dx.doi.org/10.1111/j.1365-2958.2010.07424.x>.

[16] Baitin, D.M., Gruenig, M.C. and Cox, M.M. (2008) SSB antagonizes recX–recA interaction. *J. Biol. Chem.* 283 (21), 14198–14204, <http://dx.doi.org/10.1074/jbc.M801511200>.

[17] Gruenig, M.C., Stohl, E.A., Chitteni-Pattu, S., Seifert, H.S. and Cox, M.M. (2010) Less is more: *Neisseria gonorrhoeae* recX protein stimulates recombination by inhibiting recA. *J. Biol. Chem.* 285 (48), 37188–37197, <http://dx.doi.org/10.1074/jbc.M110.171967>.

[18] Galvão, C., Souza, E., Etto, R., Pedrosa, F., Chubatsu, L., Yates, M., Schumacher, J., Buck, M. and Steffens, M. (2012) The recX protein interacts with the recA protein and modulates its activity in *Herbaspirillum seropedicae*. *Braz. J. Med. Biol. Res.* 45, 1127–1134.

[19] Berman, H., Henrick, K. and Nakamura, H. (2003) Announcing the worldwide protein data bank. *Nat. Struct. Biol.* 10 (12), 980, <http://dx.doi.org/10.1038/nsb1203-980>.

[20] Berman, H.M., Westbrook, J., Feng, Z., Gilliland, G., Bhat, T.N., Weissig, H., Shindyalov, I.N. and Bourne, P.E. (2000) The Protein Data Bank. *Nucleic Acids Res.* 28 (1), 235–242, <http://dx.doi.org/10.1093/nar/28.1.235>.

[21] Abagyan, R., Totrov, M. and Kuznetsov, D. (1994) ICM: a new method for protein modeling and design: applications to docking and structure prediction from the distorted native conformation. *J. Comput. Chem.* 15 (5), 488–506, <http://dx.doi.org/10.1002/jcc.540150503>.

[22] Abagyan, R. and Totrov, M. (1994) Biased probability Monte Carlo conformational searches and electrostatic calculations for peptides and proteins. *J. Mol. Biol.* 235 (3), 983–1002, <http://dx.doi.org/10.1006/jmbi.1994.1052>.

[23] Lindahl, E., Hess, B. and van der Spoel, D. (2001) Gromacs 3.0: a package for molecular simulation and trajectory analysis. *Mol. Model.* Annual 7 (8), 306–317, <http://dx.doi.org/10.1007/s008940100045>.

[24] Van Der Spoel, D., Lindahl, E., Hess, B., Groenhof, G., Mark, A.E. and Berendsen, H.J.C. (2005) Gromacs: fast, flexible, and free. *J. Comput. Chem.* 26 (16), 1701–1718, <http://dx.doi.org/10.1002/jcc.20291>.

[25] Hess, B., Kutzner, C., van der Spoel, D. and Lindahl, E. (2008) Gromacs 4: algorithms for highly efficient, load-balanced, and scalable molecular simulation. *J. Chem. Theory Comput.* 4 (3), 435–447, <http://dx.doi.org/10.1021/ct700301q>.

- [26] Pronk, S., Pli, S., Schulz, R., Larsson, P., Bjelkmar, P., Apostolov, R., Shirts, M.R., Smith, J.C., Kasson, P.M., van der Spoel, D., Hess, B. and Lindahl, E. (2013) Gromacs 4.5: a high-throughput and highly parallel open source molecular simulation toolkit. *Bioinformatics* 29 (7), 845–854, <http://dx.doi.org/10.1093/bioinformatics/btt055>.
- [27] Lindorff-Larsen, K., Piana, S., Palmo, K., Maragakis, P., Klepeis, J.L., Dror, R.O. and Shaw, D.E. (2010) Improved side-chain torsion potentials for the Amber ff99SB protein force field. *Proteins Struct. Funct. Bioinformatics* 78 (8), <http://dx.doi.org/10.1002/prot.22711>.
- [28] Jorgensen, W.L., Chandrasekhar, J., Madura, J.D., Impey, R.W. and Klein, M.L. (1983) Comparison of simple potential functions for simulating liquid water. *J. Chem. Phys.* 79 (2), 926–935, <http://dx.doi.org/10.1063/1.445869>.
- [29] Shvetsov, A., Schmidt, A., Lebedev, D. and Isaev-Ivanov, V. (2013) Method for calculating small angle neutron scattering spectra using all atom molecular dynamics trajectories. *J. Surf. Invest. X ray Synchrotron Neutron Tech.* 7 (6), 1124–1127, <http://dx.doi.org/10.1134/S1027451013060372>.
- [30] Feigin, L. and Svergun, D. (1987) *Structure Analysis by Small-Angle X-Ray and Neutron Scattering*, Plenum Press/Springer.
- [31] Sears, Y.F. (1992) Neutron scattering lengths and cross section. *Neutron News* 3 (3), 26–37.
- [32] Baitin, D.M., Bakhlanova, I.V., Chervyakova, D.V., Kil, Y.V., Lanzov, V.A. and Cox, M.M. (2008) Two reca protein types that mediate different modes of hyperrecombination. *J. Bacteriol.* 190 (8), 3036–3045, <http://dx.doi.org/10.1128/JB.01006-07>.
- [33] Alexseyev, A.A., Baitin, D.M., Kuramitsu, S., Ogawa, T., Ogawa, H. and Lanzov, V.A. (1997) A recombinational defect in the c-terminal domain of *Escherichia coli* reca2278-5 protein is compensated by protein binding to atp. *Mol. Microbiol.* 23 (2), 255–265, <http://dx.doi.org/10.1046/j.1365-2958.1997.1961557.x>.
- [34] Chervyakova, D., Kagansky, A., Petukhov, M. and Lanzov, V. (2001) [I29m] substitution in the interface of subunit–subunit interactions enhances *Escherichia coli* reca protein properties important for its recombinogenic activity. *J. Mol. Biol.* 314 (4), 923–935, <http://dx.doi.org/10.1006/jmbi.2001.5170>.
- [35] Craig, N.L. and Roberts, J.W. (1981) Function of nucleoside triphosphate and polynucleotide in *Escherichia coli* reca protein-directed cleavage of phage lambda repressor. *J. Biol. Chem.* 256 (15), 8039–8044.
- [36] Dudkina, A., Shvetsov, A., Bakhlanova, I. and Baitin, D. (2011) Change of filamentation dynamics of reca protein induced by d112r amino acid substitution or atp to datp replacement results in filament resistance to recx protein action. *Mol. Biol.* 45, 500–507, <http://dx.doi.org/10.1134/S0026893311030046>.
- [37] Garmay, Y., Shvetsov, A., Karelov, D., Lebedev, D., Radulescu, A., Petukhov, M. and Isaev-Ivanov, V. (2012) Correlated motion of protein subdomains and large-scale conformational flexibility of reca protein filament. *J. Phys. Conf. Ser.* 340 (1), 012094, <http://dx.doi.org/10.1088/1742-6596/340/1/012094>.
- [38] VanLoock, M.S., Yu, X., Yang, S., Galkin, V.E., Huang, H., Rajan, S.S., Anderson, W.F., Stohl, E.A., Seifert, H. and Egelman, E.H. (2003) Complexes of reca with lexa and recx differentiate between active and inactive reca nucleoprotein filaments. *J. Mol. Biol.* 333 (2), 345–354, <http://dx.doi.org/10.1016/j.jmb.2003.08.053>.
- [39] Svergun, D.I., Richard, S., Koch, M.H.J., Sayers, Z., Kuprin, S. and Zaccai, G. (1998) Protein hydration in solution: experimental observation by X-ray and neutron scattering. *Proc. Natl. Acad. Sci.* 95 (5), 2267–2272.